Primary research

Mechanisms of suberoylanilide hydroxamic acid inhibition of mammary cell growth

Thenaa K Said, Ricardo CB Moraes, Raghu Sinha and Daniel Medina

Department of Molecular and Cellular Biology, Baylor College of Medicine, Houston, Texas, USA

Correspondence: Thenaa K Said, Department of Molecular and Cellular Biology, Baylor College of Medicine, Houston, TX 77030, USA. Tel: +1 713 798 4834; fax: +1 713 790 0545; e-mail: tsaid@bcm.tmc.edu

Received: 26 July 2000
Revisions requested: 30 August 2000
Revisions received: 17 October 2000
Accepted: 6 November 2000
Published: 22 December 2000

Breast Cancer Res 2001, **3**:122–133

(Print ISSN 1465-5411; Online ISSN 1465-542X)

Abstract

The mechanism of suberoylanilide hydroxamic acid in cell growth inhibition involved induction of pRb-2/p130 interaction and nuclear translocation with E2F-4, followed by significant repression in E2F-1 and PCNA nuclear levels, which led to inhibition in DNA synthesis in mammary epithelial cell lines.

Keywords: cell growth inhibition, mammary epithelial cells, suberoylanilide hydroxamic acid

Synopsis

Background: Hybrid polar compounds (HPCs) have induced cell growth arrest, terminal differentiation and/or apoptosis in various transformed cell lines. We have previously reported that the prototype HPC (hexamethylene bisacetamide [HMBA]) was able to arrest the growth of transformed mammary (TM) 2H cells (p53 null), a highly tumorigenic mouse mammary epithelial cell line, by inhibiting G1 kinase activities, concomitant with an increase in the cyclin D2 protein level and hypophosphorylated isoforms of the three pRb pocket proteins, which led to the formation of stable cyclin D2/pRb complexes and G1 cell arrest. It has been reported that the second generation of HPCs (suberoylanilide hydroxamic acid [SAHA]), structurally related to but 2000-fold more potent than HMBA, was an inhibitor of histone deacetylase activity and caused accumulation of hyperacetylated histone H4 in murine erythroleukemia.

Objectives: To determine the mechanism of SAHA in cell growth inhibition in TM10 (p53 wt) and TM2H (p53 null) hyperplastic mouse mammary cell lines.

Methods: TM10 and TM2H cells were examined in the presence or absence of 2.5 μM SAHA for cell growth rate by [^{3}H]-thymidine uptake, DNA synthesis by flow cytometry after cells were labeled with BrdU, G1/S cyclin-dependent kinase (cdk) activities, phosphorylation levels of pRb pocket proteins, protein levels of E2F-1, PCNA and p21, pRb-2/p130 interaction, and nuclear localization with E2F-4 by western blot, immunoprecipitation and immunostaining assays.

Results: SAHA was able to arrest cell growth at G1, and inhibited DNA synthesis in both TM10 and TM2H cell lines. Cell growth arrest was accompanied by increases in histone H3 and H4 protein and acetylation levels, a profound increase in the interaction and nuclear localization of pRb-2/p130–E2F-4 complexes, significant reductions in E2F-1 and PCNA protein levels, inhibition in G1/S cdk activities and increases in the levels of hypophosphorylated isoforms of three pRb pocket proteins.

Conclusion: A novel mechanism of SAHA mediated growth inhibition through significant increases in the formation and nuclear localization of pRb-2/p130–E2F-4 complexes, which resulted in cell growth arrest and significant repression in the levels of two key molecules, E2F-1 and PCNA, essential for DNA synthesis in two mouse mammary epithelial cell lines. These responses to SAHA were independent of the p53 status of the cell; however, reversibility of SAHA-mediated growth correlated with the wild type p53 status.

cdk = cyclin-dependent kinase; EGF = epidermal growth factor; HDAC = histone deacetylase; FITC = fluorescein isothiocyanate; HMBA = hexamethylene bisacetamide; HPC = hybrid polar compounds; PBS = phosphate buffered saline; ppm = parts per million; Rb = retinoblastoma protein; SAHA = suberoylanilide hydroxamic acid; TM = transformed mammary.

Introduction

Progression through the mammalian cell cycle requires that gene expression is coordinated with the activity of cell cycle control proteins. A critical period is the transition from the G1 into the S phase, as cells become committed to the division cycle. Binding of free E2F/DP heterodimers to E2F sites generally activates transcription of proteins required for G1 → S transition and DNA synthesis [1–5], whereas complex formation with pRb or other pocket proteins including p107 and pRb-2/p130 silences transcriptional activities of downstream target genes [6–10]. The resulting retinoblastoma protein (Rb)–E2F interaction not only blocks transcriptional activation by E2F, but also forms an active transcriptional repressor complex at the promoter of cell cycle genes that can block transcription by recruiting histone deacetylase (HDAC) and remodeling chromatin [11–14].

Several HDAC inhibitors mediate cell growth arrest and/or differentiation [15–17]. We chose to examine the effect of HPCs, which have been reported to induce terminal differentiation and/or apoptosis [18–20] in many transformed cells. Although treatment with HMBA induces remission in patients with myelodysplastic syndrome and acute myelogenoud leukemia, it is not currently used therapeutically because of the high dosage required (millimolar blood levels) and the accompanying toxic side effects (thrombocytopenia) [21].

In this study, we report a novel mechanism of cell growth inhibition by the second generation of HPCs, named SAHA, which is 2000-fold more potent than HMBA and bears at least one hydroxamide in place of the amides in HMBA [17]. SAHA was reported to be a histone deacetylase inhibitor and caused accumulation of hyperacetylated histone H4 in murine erythroleukemia [17]. Very little is known about the anticancer mechanism of SAHA in epithelial cells; however, a recent study demonstrated that SAHA diet, at 900 parts per million (ppm), fed to rats reduced methylenitrosouren-induced mammary tumor incidence by 40%, total tumors by 66% and tumor volume by 78% [22]. In this study, we tested whether SAHA has similar potency to inhibit cell growth in two mouse mammary epithelial cell lines, TM10 (p53 wt) and TM2H (p53 null). We identified a novel mechanism for SAHA in cell growth arrest through inhibition in DNA synthesis, concomitant with significant increases in the nuclear localization of pRb-2/p130 associated with E2F-4, decreases in key molecules in DNA synthesis (E2F-1, PCNA and p21), and increases in histone H3 and H4 protein and acetylation levels. This study discusses the difference in recovery from cell growth inhibition in two mammary epithelial cell lines, TM10 and TM2H, after SAHA removal from cultures.

Materials and methods

Development of cell lines and cell culture

The TM10 and TM2H cell lines chosen for this study were isolated from two different mouse mammary hyperplastic outgrowths: TM10 and TM2H, respectively, as described earlier [23]. The parental TM10 outgrowth is a moderately tumorigenic outgrowth line *in vivo* (time for 50% of the transplants to produce tumors, 11 months) that is karyotypically diploid and maintains wild type p53 expression. TM2H, in contrast, is a highly tumorigenic outgrowth line *in vivo* (time for 50% of the transplants to produce tumors, ≤4 months), karyotypically aneuploid (DNA index = 1.69) and contains a p53 mutation resulting in a null phenotype [24]. Exponentially growing TM10 and TM2H cell lines in DMEM/F12 media buffered with 10 mM HEPES at pH 7.6 with 2% adult bovine serum, 10 μg/ml insulin, 5 ng/ml epidermal growth factor (EGF) and 5 μg/ml gentamycin at 60–70% confluence were treated with SAHA (courtesy of Dr Paul Marks and Dr Victoria Richon, Memorial Sloan Kettering Cancer Center, New York, NY, USA). Cells were examined at the time points indicated for cell growth and cell cycle activities.

Analysis of cell growth

Cell growth rates of TM10 and TM2H lines were determined using a [^{3}H]-thymidine uptake assay, as described earlier [25]. In initial studies, both cell lines were cultured in the absence or presence of 0.1, 2.5, 5.0, and 10 μM SAHA for 6 days. Both cell lines were also cultured for 2 days in the presence of SAHA at the concentrations already mentioned, followed by removing SAHA from the media for a subsequent 4 days. Based on the results of these studies, subsequent experiments examined asynchronously growing TM10 and TM2H cell lines in the presence or absence of 2.5 μM SAHA for 24 h.

FACS analysis

Exponentially growing cells at 60–70% confluence at control or treated with 2.5 μM SAHA for 24 h were pulse-labeled for 1 h with 10 μM BrdU (Sigma, St Louis, MO, USA). The cell cultures were rinsed once with phosphate buffered saline (PBS), trypsinized for 3 min and rinsed three times with PBS. Cells were resuspended in 200 μl PBS and fixed in 5 ml cold 70% ethanol overnight. Fixed cells were counted and, generally, 4×10^6 cells were transferred to 15 ml polypropylene tubes, centrifuged at 3000 rpm for 5 min and the supernatant removed. Cells were stained for the newly incorporated BrdU for DNA synthesis using BrdU monoclonal antibodies conjugated to fluorescein isothiocyanate (FITC) and stained with propidium iodide for DNA content following the protocol described in Becton and Dickinson's (San Diego, CA, USA) instructions for flow cytometric analysis.

Nuclear and cytoplasmic extracts

To obtain nuclei, (4–6) × 10^7 cells of each cell line grown in the presence and absence of 2.5 μM SAHA were washed twice in PBS, followed by suspension in 0.3 ml nuclear buffer consisting of 2 mM $MgCl_2$, 5 mM K_2HPO_4, 0.1 mM EDTA, 1 mM PMSF, 20 μg/ml aprotinin, 20 μg/ml leupeptin, 0.1 mM Na_3VO_4 and 5 mM β-glycerophosphate. An additional 0.3 ml nuclear buffer containing 0.7% Triton X-100 was then added, after standing on ice for 8–10 min. The suspensions were examined for cell lysis microscopically, centrifuged at 800 rpm for 10 min at 4°C, and the supernatant designated the cytoplasmic fraction. The pellets were washed once with nuclear buffer, and the nuclear extracts were prepared by resuspending the pellets in 0.3 ml buffer containing 20 mM HEPES (pH 7.8), 25% glycerol, 0.42 M NaCl, 1.5 mM $MgCl_2$, 0.2 mM EDTA, 0.5 mM PMSF, 0.5 mM DTTl, 0.1 mM Na_3VO_4, 50 mM NaF, 20 μg/ml leupeptin, and 5 mM β-glycerophosphate. Sonication was carried out on ice using an ultrasonicator processor (PGC Scientific, Caithersburg, MA, USA), and the mixtures were examined microscopically for complete break of the nuclei. The supernatants were designated as nuclear extracts after centrifugation of the mixtures, and the total protein was determined in the nuclear and cytoplasmic fractions.

Western blot and immunoprecipitation analysis

Histones were isolated and lyophilized from nuclear extracts in SAHA treated and untreated TM10 and TM2H cell lines following a protocol described earlier [26]. Histone samples were assessed for purification quality on 15% SDS acrylamide gel including calf thymus histones as controls before western blot analysis was carried out. Histone samples were resolved by electrophoresis using 15% acid–urea gel containing 36% w/v urea, 5% v/v acetic acid, 600 μl TEMED and 0.7 ml of 10% ammonium persulfate prepared as described elsewhere [27]. Gels were either stained by Coomassie Brilliant Blue or equilibrated to be transferred into transfer buffer (0.7% acetic acid). The gel sandwich was set up as usual except for the placement of the blotting membrane (because proteins in this type of gel will migrate toward the negative electrode), and the procedure was continued as described earlier [27]. Each histone was resolved into multiple bands and were visualized in Coomassie blue gel. The acetylated histone isoforms were detected by immunoblot against acetylated histone H3 isoforms using anti-H3 antibodies raised and characterized by Dr Sharon Roth at MD Anderson Cancer Center (personal communication) or against acetylated histone H4 isoforms using anti-H4 polyclonal antibody (Upstate Biotechnology Inc, Lake Placid, NY, USA).

Western blot analysis for all the proteins examined in this study was carried out on equal amounts of cellular fraction protein extracts (100 μg/sample) following a protocol described earlier [25]. Staining the gel with Coomassie Brilliant Blue for each experiment assessed equal loading control. TM10 and TM2H cells (0.65 × 10^3 cells/cm^2) seeded in 75 T flasks grew for 2 days, and were treated with 2.5 μM SAHA for 24 h. Cellular fraction protein extracts were prepared after SAHA treatment [25]. Primary antibodies used at 1 or 2 μg/ml were p21/Cip (Pharmingen Inc, San Diego, CA, USA), pRb (IF8), p107 (SD9), p130 (C-20), E2F-1 (C-20), E2F-4(C-20) and PCNA (C-20) (Santa Cruz Biotechnology Inc, Santa Cruz, CA, USA). All antibodies were examined for specificity prior to use. The secondary antibodies conjugated to horseradish peroxidase (1 : 5000–1 : 15,000 dilution) were used followed by enhanced chemiluminescence detection reaction as described by the manufacturer (Amersham Pharmacia Biotechnology, Amersham, Bucks, UK).

The immunoprecipitation assay followed by western blot analysis was as described previously [25]. Briefly, equal nuclear cell extract (200 μg/sample) was mixed with 3 μg anti-E2F-4 antibodies at 4°C followed by the addition of 50 μl protein A-sepharose beads (Amersham Biotechnology). The immune complex was centrifuged, and the proteins in the immune complex were resolved by 10% SDS-PAGE followed by western blot analysis using anti-pRb-2/p130 antibodies as already described for western blot analysis.

Cyclin-dependent kinase assay

The TM10 and TM2H cell cultures at control and treated with 2.5 μM SAHA for 24 h were examined for cyclin D1, E, and A associated kinase activities as described previously [28]. Briefly, cellular protein extracts (25 μg) were precleared with 10 μl of 10% preimmune normal rabbit serum followed by immunoprecipitation with either 3 μg anti-cyclin D1, E polyclonal antibodies (Upstate Biotechnology), 2 μg anti-cyclin A polyclonal antibody antibodies (C-19)-G (Pharmingen), or normal rabbit preimmune serum as a negative control. All antibodies were examined for specificity [28]. Immunoprecipitate complexes were examined for kinase assay following a procedure described previously [28]. The substrates utilized in the kinase assays were either Histone-H1 (Sigma) or RB protein (Santa Cruz Biotechnology). The phosphorylated H1 and pRb bands were scanned and quantitated densitometrically using a Phosphoimager (Molecular Dynamics, Sunnyvle, CA, USA).

Immunofluorescent staining

Exponentially growing cells on slides were fixed in 4% paraformaldehyde in PEM buffer (80 mM Pipes [pH 7.0], 5 mM EGTA and 2 mM $MgCl_2$) for 30 min, permeabilized in 0.5% Triton X-100 in PEM buffer at room temperature for 15 min and rinsed three times with TBS + 0.1% Tween 20, followed by incubation in 0.5% nonfat dry milk in TBS + 0.1% Tween 20 for 2 h at room temperature.

Figure 1

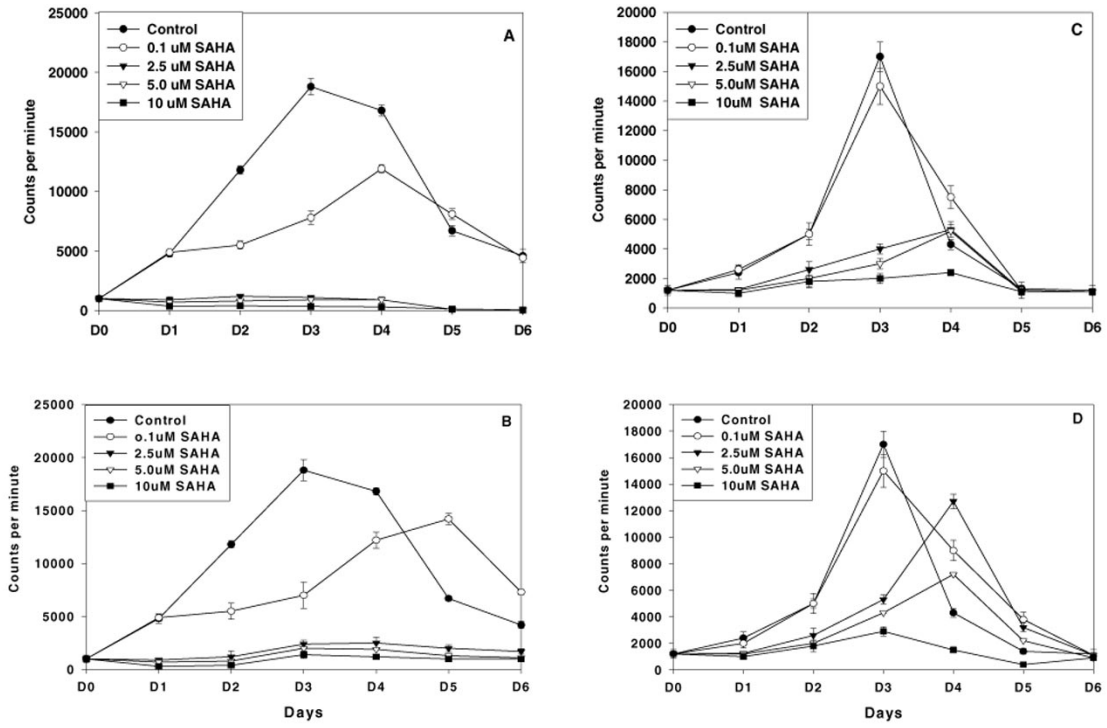

Dose effect of SAHA on growth rate in TM10 and TM2H cell lines. **(A)**, **(C)** Growth curves for TM10 and TM2H cell lines in the absence and presence of 0, 0.1, 2.5, 5.0, and 10 μM SAHA. **(B)**, **(D)** Growth curves in the absence and presence of the same SAHA concentrations as (A) and (C) for 2 days, and then SAHA was removed from the media for the four following days. Each point is the average of four readings.

For BrdU and DAPI double immunostaining, cells were incubated for 30 min in media supplemented with 5 μM BrdU. After 30 min, cells were incubated in 2 N HCl for 5 min at room temperature prior to incubation with the primary antibody (this step was omitted for pRb-2/p130 immunostaining). Following washing three times, cells were incubated in a (1 : 50) dilution of mouse anti-BrdU monoclonal antibody (Boehringer Mannheim, Indianapolis, IN, USA) for 2 h at 37°C. After washing three times, cells were then incubated in FITC-conjugated anti-mouse secondary antibody (1 : 400) dilution for 1 h at 37°C, followed by washing three times with anti-fade equilibrating buffer and mounting in anti-fade mounting medium (Molecular Probe, Eugene, OR, USA). The same sequential steps were followed for pRb-2/p130 immunostaining using anti-pRb-2/p130 monoclonal antibodies (Santa Cruz Biotechnology).

Apoptosis

Apoptotic activities in TM10 and TM2H cells in the absence and presence of 2.5 μM SAHA were examined by two procedures: the TACS 2TdT *In Situ* Apoptosis Detection assay following the manufacturer's instructions (Trevingen, Gaithersburg, MD, USA), and the DNA Fragmentation Assay described elsewhere [29].

Results

Effect of SAHA on TM10 and TM2H cell proliferation and morphology

The TM10 and TM2H cell lines were used to investigate whether the status of p53 influences the outcome of SAHA treatment. The origin of TM10 and TM2H cell lines was described earlier [30]. The rate of cell proliferation at concentrations of 0, 1.0, 2.5, 5, and 10 μM SAHA was examined by [^{3}H]-thymidine assay at the indicated time points. The inhibitory effect of SAHA at concentrations of 2.5 μM and higher on cell proliferation was profound on both cell lines after 24 h. The TM10 cell proliferation continued to be inhibited during the following 5 days in the presence of SAHA, whereas minimal growth in TM2H cell growth on days 3 and 4 was observed (Figs 1A,C). After removing SAHA from the cultures following 2 days of exposure to all SAHA concentrations, TM10 cells continued to be inhibited at concentrations of 2.5 μM and higher during the following 4 days of SAHA free cultures (Fig. 1B), whereas TM2H cells resumed proliferation (Fig. 1D). These results suggest that SAHA induced a dose-dependent block in DNA replication on both cell lines. A 2.5 μM dose of SAHA was used in further experiments because this concentration seems to be unequivocally effective on cell growth inhibition on both cell lines

after 24 h of treatment. Furthermore, no apoptotic activity was observed after 24 and 48 h of treatment with 2.5 μM SAHA in both cell lines (data not shown).

The effect of SAHA on blocking cell proliferation through blocking DNA synthesis was examined by BrdU labeling, as determined by immunofluorescence staining (Fig. 2A), and the cell cycle profile by flow cytometric analysis (Fig. 2B). The BrdU indices in the control TM10 and TM2H cells, including all types of BrdU staining patterns, were 16 and 34%, respectively, indicating that the percentage of TM2H cells synthesizing DNA or in the 'S phase' were more than double that of TM10 cells (Fig. 2A). Upon 2.5 μM SAHA treatment for 24 h, 800 cells per sample were counted stained with BrdU against cells stained with DAPI, and BrdU labeling indices dropped dramatically to 4 and 6% in TM10 and TM2H cells, respectively. Furthermore, the BrdU staining revealed the size and pattern of replication clusters, which are related to the general patterns of DNA replication in mammalian cell nuclei at early, mid and late S phase [31]. These data suggested that 2.5 μM SAHA was capable of inhibiting cell proliferation in both TM10 and TM2H cell lines by blocking DNA synthesis, regardless of their differences in the number of cells synthesizing DNA.

These results were confirmed by flow cytometric analysis after staining cells with BrdU for newly synthesized DNA and with propidium iodide for DNA content. The percentages of cells in the G1 and S phases in control TM10 cells at the time of treatment were 57 and 18%, respectively, and those for TM2H cells were 39 and 28%, respectively (Fig. 2B). The number of TM2H cells growth arrested in the G1 phase upon SAHA treatment for 24 h increased by 21%, compared with the 8% increase in the TM10 cell line, concomitant with similar differences in the percentage of cells inhibited in the S and G2/M phases (Fig. 2B). This difference in G1 cell growth arrest between the two cell lines may be attributed to their differences in the initial number of cells distributed in each cell cycle phase before treatment.

The shape and morphology of TM10 and TM2H cells grown on slides in the presence and absence of 2.5 μM SAHA were examined. The dimensions of 50 randomly selected cells of each cell line were measured using a microscope scale. The TM10 and TM2H mammary epithelial cells measured 5.4 ± 2.1 and 3.6 ± 1.4 μm in width and 13.7 ± 5.9 and 18.6 ± 8.0 μm in length, respectively. TM10 cells generally had five to seven extensions, whereas TM2H cells had three to five extensions. TM10 and TM2H cells became flattened and increased in both nuclear and cytoplasmic volume after 24 h of 2.5 μM SAHA treatment. Both cells exhibited less distinct intracellular borders (Fig. 3). The morphology of both cell lines was similar to cells committed to cell differentiation; however, these mammary cells grown on plastic dishes were unable to differentiate by SAHA.

Figure 2

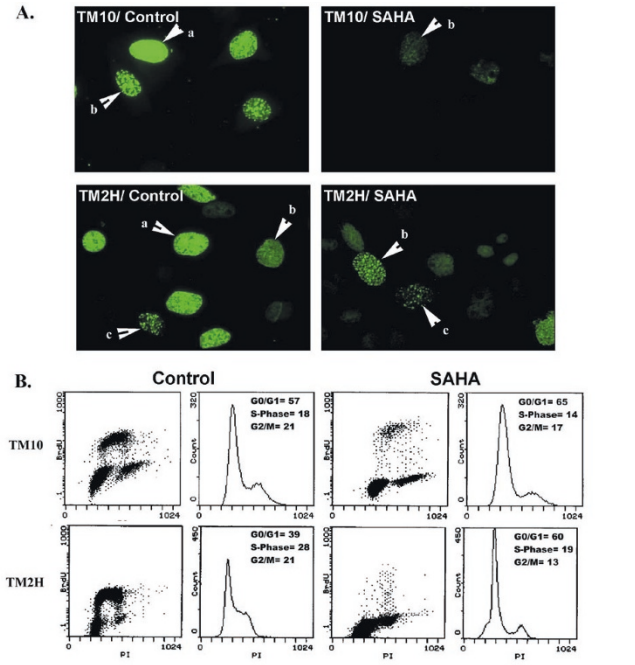

Effect of SAHA on cell growth properties of TM10 and TM2H preneoplastic mammary cells. **(A)** BrdU immunostaining of TM10 and TM2H cells at control or treated with 2.5 μM SAHA for 24 h. **(B)** Flow cytometric analysis of TM10 and TM2H cell lines at the same conditions as (A) were analyzed for BrdU fluorescence and DNA content. Histograms of cell cycle distribution were calculated from a sample of 5000 events.

Effect of SAHA on histone protein and acetylation levels in TM10 and TM2H cell lines

It is not known whether SAHA alters the protein acetylation levels of various histones in the mammary epithelial cells. Changes in the acetylation or phosphorylation of histones result in alterations that can be visualized as changes in protein mobility on an acid–urea gel following western blot analysis [26,27]. These gels separate histones on the basis of charges as well as size, resulting in multiple bands for each histone that correspond to differently modified isoforms. These isoforms can be identified by their characteristic mobility and by staining with antibodies specific to each histone isoform [26]. Protein and acetylation levels of histone H3 and H4 isoforms on histone samples isolated from SAHA treated and untreated TM10 and TM2H cells stained by Coomassie Brilliant Blue (Fig. 4A) and by western blots (Fig. 4B) were examined to identify the potency of SAHA as a histone deacetylase inhibitor on mammary epithelial cells. We focused on H3 and H4 because antibodies are available and acetylation events in those histones have been

Figure 3

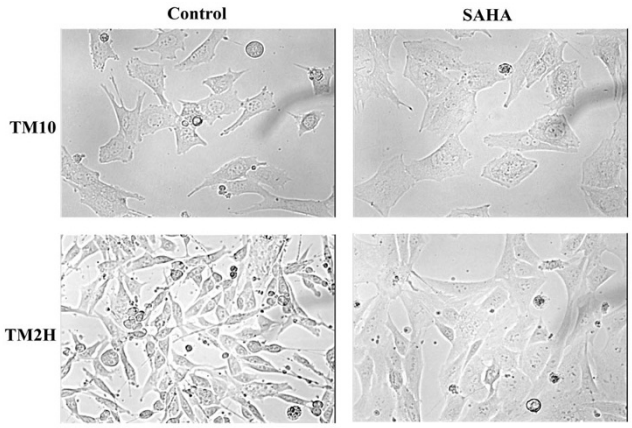

Effect of SAHA on TM10 and TM2H morphology. Bright field pictures for living TM10 and TM2H cells at control and in SAHA treated conditions for 24 h taken at 40× magnification.

studied. These results suggested that SAHA not only increased histone acetylation, as shown in H4 (Fig. 4A), but also increased histone protein levels in TM10 and TM2H cells (Fig. 4B). The increases in protein and acetylation levels of H3 and H4 in SAHA treated TM10 and TM2H cell lines were indicated by the strong staining with the acetylation specific antibodies of H3 and H4, while the acetylated slow migrated isoforms showed smearing due to the increases in their protein level (Fig. 5B). We did not, however, observe differences in the initial acetylation levels between untreated TM10 and TM2H cell lines.

SAHA induced hypophosphorylation of all the three pocket proteins

Phosphorylation of three major pocket proteins, Rb, p107 and Rb2/p130, were examined after SAHA treatment, as each pocket protein affects the G1 and S phases of the cell cycle. Upon treatment with 2.5 μM SAHA for 24 h, a profound increase in hypophosphorylation of the three pocket proteins was observed in both TM10 and to a lesser extent in TM2H cells as compared with their control counterparts, judged by the faster mobility of the Rb pocket protein isoforms on SDS gel (Fig. 5). The difference in the level of hypophosphorylated pRb pocket protein isoforms between the two cell lines treated with SAHA may be attributed to differences in G1 and S phase cdk activity (examined in the following section). Results suggested that SAHA induced cell growth arrest through dephosphorylation of three pRb pocket proteins, which may be related to inhibition in G1/S phase cdk activities.

SAHA inhibits multiple cyclin-associated kinase activities

There are extensive studies on the relation between specific phosphorylation sites on pRb and its potential

Figure 4

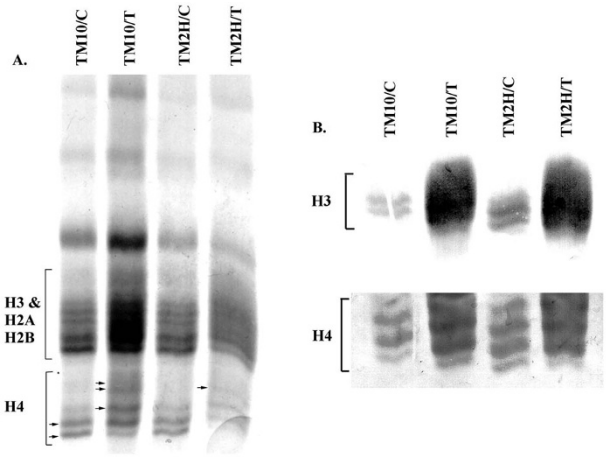

Effect of SAHA on histone protein and acetylation levels. **(A)** Equal amounts of isolated and purified histone samples from TM10 and TM2H nuclei at control (C) and treated with 2.5 μM SAHA for 24 h (T) were resolved on 15% acid–urea gel and stained with Coomassie Blue. **(B)** Western blot analyses of the same samples in (A) were analyzed, using 15% acid–urea gel, equilibrated to be transferred on nitrocellulose membrane, probed first with anti-H3 polyclonal antibody, striped and re-probed with anti-H4 polyclonal antibodies. Acetylated histone H4 of multiple bands (arrows) was revealed as slow migrating bands in treated versus control samples after Coomassie blue staining, while H3 showed smear of the bands attributed to an increase in both acetylation and protein synthesis. The increase in histones H3 and H4 protein and acetylation levels showed intense smeared bands after alkaline phosphatase colorimetric reaction.

Figure 5

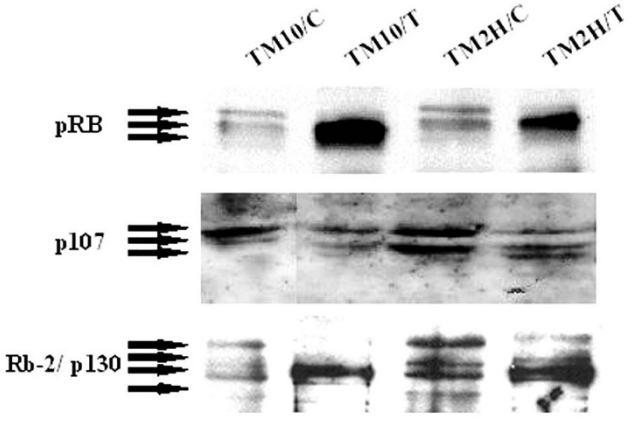

Effect of SAHA on phosphorylation levels of the pRb pocket proteins. Western blot analysis of 100 μg nuclear protein extracts of TM10 and TM2H cell lines in control (C) or treated with 2.5 μM SAHA for 24 h (T). Protein samples were resolved by 10% SDS-PAGE, transferred onto nitrocellulose membrane, blocked and probed with antibodies against pRb, p107 and Rb-2/p130 as described in Materials and methods. Note the fast migrating and more intense Rb, p107 and Rb-2/p130 'hypophosphorylated forms' in SAHA treated (T) versus control (C) cell lines.

Figure 6

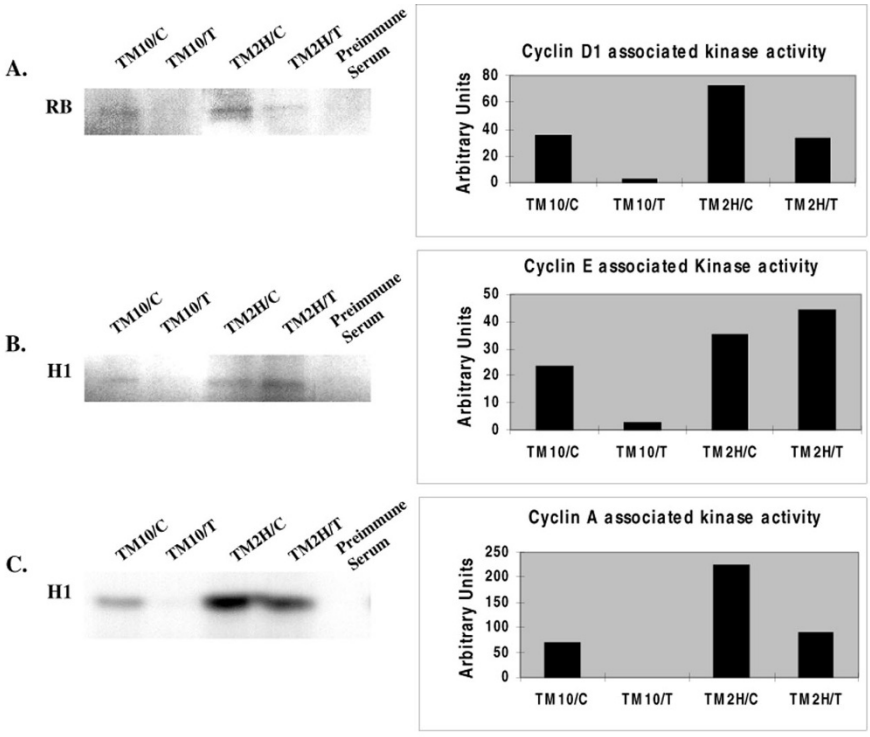

Effect of SAHA on cyclin-associated kinase activities in TM10 and TM2H cells. Equal amounts of nuclear protein extracts (250 μg) from TM10 and TM2H cells at control (C) and treated with 2.5 μM SAHA for 24 h (T) were immunoprecipitated with antibodies against anti-cyclin D1 (**A**), anti-cyclin E (**B**) and anti-cyclin A (**C**) or with rabbit preimmune serum, followed by kinase activity assay, as described in Materials and methods. The negative control in each panel was 250 μg protein extract from TM2H cells at control condition immunoprecipitated with rabbit preimmune serum. The phosphorylated substrates, pRb and histone (H1), were scanned and quantitated densitometricaly using a phosphoimager analyzer. Histograms represent arbitrary units of the phosphorylated substrates after subtracting the background and the negative control.

transcription repression [32–34]. It is well known that pRb phosphorylation sites are recognized by specific cdks [33], and that most of the 16 pRb-phosphorylation sites are sequentially phosphorylated throughout the cell cycle (reviewed in [34,35]). SAHA treatment resulted in G1 cell growth arrest in TM10 and TM2H cell lines, concomitant with the profound increase in dephosphorylation of the three pRb pocket proteins. Therefore, we examined cyclin D1, E and A cdk2 activities in TM10 and TM2H cell cultures after 24 h treatment with SAHA because they reflect kinase activities before, during and after the G1 → S checkpoint, respectively. The three cyclin/cdk2 complexes directly reflect the sequential events in DNA synthesis [36]. The initial levels of cyclin D1, E and A associated kinase activities were 3-, 2.5- and 4-fold higher in untreated TM2H compared with TM10 cells, respectively (Fig. 6A–C). These results were predicted based on their differences in cell distribution throughout the cell cycle, as appeared in the cell cycle profile analysis, and may reflect the cell line differences in known p53 status. Cyclin D1, E and A associated kinase activities decreased by four-, four-, and fivefold, respectively, in TM10 cells compared with control on SAHA treatment, whereas only cyclin D1 and A associated kinase activities decreased (2.2- and 2.6-fold, respectively) in SAHA treated TM2H cells compared with control (Fig. 6). These data demonstrate that SAHA inhibits multiple cdk activities, and the degree of inhibition was more profound in TM10 verses TM2H cells.

Effect of SAHA on p21, PCNA, E2F-1 and E2F-4 proteins as a function of cell growth inhibition

The difference in the protein level of p21/Cip1 between TM10 and TM2H cell lines was predicted based on their differences in p53 status (Fig. 7A). Perinuclear localization of p21 was detected in only few TM2H cells (p53 null) when both cell lines were immunostained for p21, whereas p21 was localized in both cytoplasmic and nuclear compartments in TM10 cells (p53 wt) (data not shown). The p21 expression level decreased by 50% in TM10 cells upon SAHA treatment (Fig. 7A). These results suggest that SAHA inhibited DNA synthesis in the presence or absence of p21 protein.

PCNA [37] and E2F-1 [1,7] are two key mediators of the G1 → S transition and DNA synthesis. Because such regulatory proteins can be present at different levels and in

Figure 7

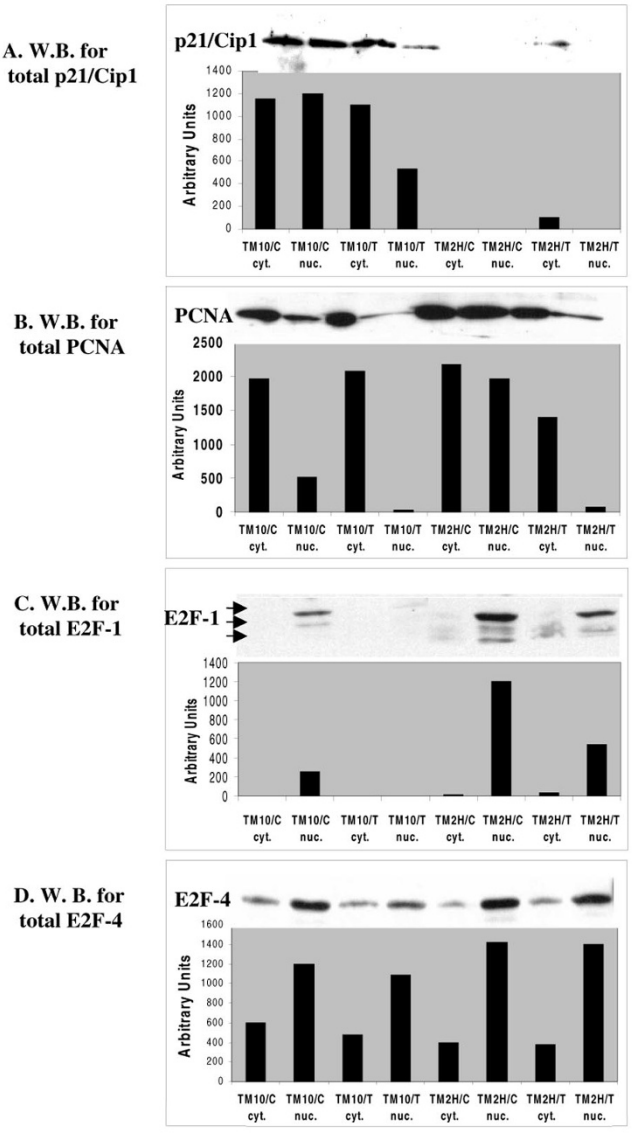

Effect of SAHA on the subcellular distribution of p21/Cip, PCNA, E2F-1 and E2F-4 in TM10 and TM2H cell lines. Equal amounts of nuclear (nuc.) and cytoplasmic (cyt.) protein extracts (100 μg) from TM10 and TM2H cells at control (C) and treated with 2.5 μM SAHA for 24 h (T) were analyzed by western blot (W.B.) using anti-mouse p21 antibody (**A**), mouse anti-PCNA antibody (**B**), rabbit anti-E2F-1 antibody (**C**) and anti-E2F-4 antibody (**D**). Protein bands were scanned and quantitated densitometricaly using a phosphoimager analyzer. Histograms represent arbitrary units for each protein.

different molecular complexes in nuclei as compared with the cytoplasm, separation of the two cellular compartments allowed an assessment of the site(s) at which these proteins exert their primary activity unimpeded by artifacts that may result from intermixing the two compartments. In the untreated cells, the cytoplasmic PCNA protein levels in TM10 and TM2H cell lines were similar, but the level of PCNA in the nuclear fraction was fourfold higher in TM2H cells compared with TM10 cells (Fig. 7B). The effect of SAHA was profound on the nuclear PCNA fraction in both cell lines, but minimal on the cytoplasmic PCNA fraction. The pronounced difference in the levels of PCNA in growing versus arrested cells is in accordance with the determinant role PCNA plays in DNA synthesis [37,38].

To further investigate the effect of SAHA on inhibition of DNA synthesis, we examined E2F-1 as a key mediator for G1 → S transition and DNA synthesis. The initial nuclear protein level of E2F-1 in the untreated TM2H cells was 4.8-fold higher compared with the TM10 cell line (Fig. 7C). Nuclear E2F-1 protein was completely abolished in TM10 cells after 24 h of SAHA treatment, and decreased 2.2-fold in TM2H cells (Fig. 7C). These results demonstrate that SAHA treatment also inhibits E2F-1 protein levels.

It has been reported that expression of *E2F-4* gene does not change in relation to cell growth, although a modest increase can sometimes be observed in growing cells [39]. E2F-4 protein levels were examined in the nuclear and cytoplasmic fractions in both cell lines with and without SAHA, and the protein levels did not change upon SAHA treatment in either fractions of either cell line (Fig. 7D). It is noteworthy that the mechanism of SAHA in G1 cell growth arrest may target the expression of specific proteins involved in DNA synthesis as it inhibited E2F-1 and PCNA, but not E2F-4, suggesting that SAHA may cause different levels of histone acetylation at distinct regions of the genome.

Rb-2/p130 subcellular localization and interaction with E2F-4 was examined in both cell lines in the absence and presence of SAHA because Rb-2/p130 is an important cytoplasmic partner of E2F-4 and is capable of inducing nuclear localization of the complex upon cell growth arrest and differentiation [40,41]. Immunostaining analysis using monoclonal antibody specific for pRb-2/p130 revealed that SAHA enhanced pRb-2/p130 nuclear localization in both cell lines treated with SAHA for 24 h compared with their controls (Fig. 8A). To examine whether the increase in hypophosphorylation of pRb-2/p130 (Fig. 5) and its nuclear localization after SAHA treatment was associated with interaction to E2F-4, equal amounts of nuclear protein extracts were immunoprecipitated with antibodies against E2F-4 followed by western blot analysis against pRb-2/p130 antibodies. Interestingly, the results revealed an unequivocal increase in the nuclear pRb-2/p130 protein level associated with E2F-4 in both cell lines treated with SAHA (Fig. 8B). These intriguing results indicate that the interaction of hypophosphorylated pRb-2/p130 with E2F-4 followed by enhancement in nuclear location after SAHA treatment is a novel mechanism in SAHA-mediating cell growth arrest.

Figure 8

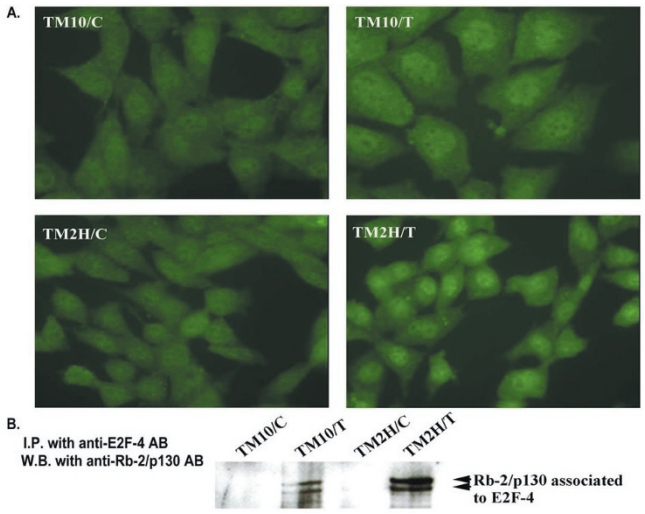

Analysis of Rb-2/p130 subcellular localization and interaction with E2F-4 in control and SAHA treated TM10 and TM2H cell lines. (**A**) Immunofluorescent staining of Rb-2/p130 in TM10 and TM2H cell lines at control (C) and treated with 2.5 μM SAHA for 24 h (T). (**B**) Nuclear protein extracts (200 μg) of both cell lines and at the same conditions as (A) were immunoprecipitated with anti-E2F-4 polyclonal antibody followed by immunoblotting with mouse anti-Rb-2/p130 monoclonal antibody. I.P., immunoprecipitation; W.B., western blot.

Table 1

The differences between TM10 and TM2H cell lines in the cell cycle profile and protein status

	TM10 cell line (p53 wt)	TM2H cell line (p53 null)
Nuclear proteins		
E2F-1	1	4.8
PCNA	1	4.0
Rb-2/p130	1 (predominantly hypophosphorylation)	1 (predominantly hypophosphorylation)
p21/Cip1	Strongly detectable	Weakly detectable
Cyclin-dependent kinase activity		
D1	1	2.2
E	1	1.7
A	1	3
BrdU index	16%	34%
Cell cycle profile		
G0/G1	57%	39%
S	18%	28%

The numbers represent fold differences between the two cell lines with the lower level designated as unity (eg 1).

Discussion

In this study, we present novel data on the mechanism of SAHA in cell growth arrest on two mouse mammary epithelial cell lines, TM10 (p53 wt) and TM2H (p53 null). SAHA was able to increase histone H3 and H4 protein and acetylation levels, and caused a profound decrease in the protein levels of key molecules, PCNA and E2F-1, essential for DNA synthesis. Furthermore, SAHA significantly enhanced the interaction of pRb-2/p130 to E2F-4 and the nuclear localization of the pRb-2/p130–E2F-4 complex. SAHA also resulted in the inhibition of G1/S kinase activities and, consequently, hypophosphorylation of the three pRb pocket proteins, which led to G1 cell growth arrest and dramatic decreases in DNA synthesis in both cell lines. TM10 cells continued to be inhibited for 4 days upon removing SAHA after 2 days of treatment, whereas TM2H cells were able to recover their proliferation potentials. A summary of the differences in the molecular status and cell cycle profile between TM10 and TM2H cell lines before SAHA treatment are summarized in Table 1. These differences in p21 protein and BrdU index were predicted based on p53 status of these two cell lines and are in parallel with other reports on mammary tumors, where the absence of p53 results primarily in greater proliferation response in the affected cell [42]. No differences in histone H3 and H4 acetylation levels were, however, observed in relation to p53 status between the two cell lines. It is not known at this point whether specific mutations of p53 alter the degree of histone acetylation in cells. Histone acetylation and p53 mutation appear not to be correlated in this study; nevertheless, it is necessary and more sensitive to examine histone acetylase and deacetylase activities in correlation to p53 status.

The mechanism of SAHA in blocking DNA synthesis, as demonstrated by flow cytometric analysis, appeared similar in both TM10 and TM2H cell lines, and implicated several events. First, SAHA increased histones H3 and H4 protein levels after 24 h of treatment, which could result in cell cycle arrest. It has been reported that upregulation of KIAA0128 gene expression, which has been implicated in activation of histone mRNA synthesis, was related to cell cycle arrest in MCF-7 cells after treatment with SAHA [43]. As SAHA treatment increased histone (H3 and H4) protein and acetylation levels in both cell lines, this may have altered the association of histones with DNA, thereby altering nucleosomal conformation and stability [27,44]. Local perturbations of chromatin structure can specifically affect the accessibility and/or function of transcriptional regulatory proteins that bind DNA sequences in the region where histone acetylation or deacetylation took place [44]. HDAC inhibitors, such as trichostatin A and trapoxin, modulate gene expression in either a positive, negative or neutral fashion [45]. Ample studies have demonstrated the implication of histone hyperacetylation in gene transcription but also in silencing gene expression of others [27,44,45].

It is well known that E2F-1 regulates transcription of genes predominantly expressed during the G1 → S transition such as cyclins [1,5], cdks [1], *E2F-1* gene [46], the *RB1* tumor suppressor gene [8,47], and genes for DNA replication and repair enzymes and factors [4]. It appears that SAHA has a profound inhibitory impact on the protein levels of key molecules, E2F-1, PCNA and p21, essential for DNA synthesis. Based on previous reports, disintegration of the cyclin/cdk complexes important for DNA synthesis is correlated to E2F-1 expression level [1,5]. It is thus conceivable to interpret that the profound inhibition in E2F-1 and PCNA protein levels after 24 h of exposure to 2.5 μM SAHA may result in disintegration and deactivation of D1, E and A cdk2 complexes, which consequently leads to hypophosphorylation of the three Rb pocket proteins. It is plausible to suggest that the inhibition in E2F-1 protein levels by SAHA was either at the transcription level or induction of the ubiquitin-protein ligase responsible for E2F-1 degradation, but not E2F-4, and this resulted in blocked DNA synthesis. Further work is necessary to prove whether the effect of SAHA is at the RNA transcription level or on stability of E2F-1 protein.

The inhibition in nuclear p21 in SAHA treated TM2H as well as TM10 cells underscores that SAHA-arrested cell growth is through a p53-independent pathway. A recent report indicated that the transcription of $p21^{Cip1}$ and accumulation of acetylated histones associated with the promoter and coding regions of that gene were induced after 2 h in 7.5 μM SAHA and fall by 24 h in T24 bladder carcinoma cells [48]. Although we have utilized 2.5 μM SAHA, our results are in agreement with their data on the fall in p21 level after 24 h of treatment.

A more intriguing and novel mechanism of SAHA-mediated cell growth arrest was the enhanced interaction and nuclear localization of Rb-2/p130–E2F-4 complexes in both cell lines after 24 h of treatment. It is well documented that E2F-1 possesses an intrinsic nuclear localization signal whereas E2F-4 is devoid of such signal [49,50], and that the mechanism of E2F-4 nuclear localization has been documented to be through its interaction with Rb-2/p130 pocket protein, which impedes cell cycle progression [39,40]. Furthermore, recent studies demonstrated that Rb-2/p130 in complexes with E2F-4 actively represses E2F-1 transcription in cell differentiation and growth arrest, and that this complex was considered the main E2F-1 regulator during the early G1 phase [39,51,52]. Other reports suggest that Rb recruitment of HDAC1 activity repressed E2F-1 [12,13]. Although SAHA increases acetylation of histones H3 and H4, it is not known whether SAHA is able to inhibit all HDAC activities of all types of histones, including HDAC1, or whether the profound increase in Rb-2/p130–E2F-4 nuclear complex after SAHA treatment may have an alternative pathway other than recruitment of HDAC1 activity.

The difference between TM10 (p53 wt) and TM2H (p53 null) cell cultures in response to removing 2.5 μM SAHA following 2 or 3 days of treatment was significant. We suggest that it might reflect their difference in p53 status. The TM10 cells did not exhibit signs of cell proliferation or 'recovery' during the following 3–4 days. TM2H cells, in contrast, recovered by 88% after 2 days of treatment. Longer treatment may be necessary to inhibit TM2H (p53 null) mammary epithelial cells as preliminary results indicate TM2H cells did not recover after 3 days of SAHA treatment (data not shown). We suggest that the difference in growth recovery between TM10 (p53 wt) and TM2H (p53 null) cell lines after 2 days in 2.5 μM SAHA may be attributed to two factors, both related to their p53 status. Firstly, the p53 in TM10 (p53 wt) cells might have been acetylated upon treatment with 2.5 μM SAHA for 2 or 3 days. Recent studies demonstrated acetylation of p53 in the C-terminal domain increased the DNA-binding capacity of the protein [53–55]. This event is obviously not present in TM2H (p53 null). Secondly, although TM10 cells (p53 wt) have lost 64% of their nuclear p21 during SAHA treatment, the remaining 36% of the nuclear p21 plus the continued synthesis of p21 by p53 activity [55–57] during the recovery period would maintain TM10 cells in the inhibited state for several days without SAHA. TM2H cells (p53 null), in contrast, lack both negative regulatory potentials of acetylated p53 and the availability of nuclear p21.

We conclude that the mechanisms of SAHA inhibition of DNA synthesis and cell growth arrest at G1 were similar in both TM10 (p53 wt) and TM2H (p53 null) mouse mammary epithelial cell lines. A proposed mechanism of SAHA stresses the involvement of pRb-2/p130–E2F-4 interaction and nuclear localization, which ultimately results in cell growth arrest and repression in nuclear E2F-1 and PCNA protein levels, and the subsequent inhibition of DNA synthesis in both cell lines. However, p53 status was critical in maintaining growth arrest in TM10 cells 4 days after removing SAHA treatment, whereas TM2H cells (p53 null) recovered growth arrest under the same conditions. We therefore suggest that the dose and time regimen for histone deacetylase inhibitors, such as SAHA, may have to consider the p53 status of breast cancers.

Acknowledgements

The authors gratefully acknowledge Dr Paul A Marks and Dr Victoria M Richon for providing us with the SAHA compound, Dr Sharon Roth for help and advice with analysis of histone acetylation level and the anti-H3 antibody, and Harry Thomas for the technical efforts on the histone acetylation experiments. This work was supported by NIH Grant CA-11944 (to DM).

References

1. DeGregori J, Kowalik T, Nevins JR: **Cellular targets for activation by the E2F1 transcription factor include DNA synthesis- and G1/S-regulatory genes**. *Mol Cell Biol* 1995, **15**:4215–4224.

2. Shan B, Farmer AA, Lee WH: **The molecular basis of E2F-1/DP-1-induced S-phase entry and apoptosis**. *Cell Growth Diff* 1996, **7**:689–697.
3. Cao L, Faha B, Dembski M, Tsai L, Harlow E, Dyson N: **Independent binding of retinoblastoma protein and p107 to the transcription factors E2F**. *Nature (London)* 1992, **355**:176–179.
4. Hsiao K-M, McMahon SL, Farnham PJ: **Multiple DNA elements are required for the growth regulation of the mouse E2F1 promotor**. *Genes Dev* 1994, **8**:1526–1537.
5. Schulze A, Zerfass K, Spitkovsky D, Middendorp S, Berges J, Helin K, Jansen-Durr P, Henglein B: **Cell cycle regulation of the cyclin A gene promoter is mediated by a variant E2F site**. *Proc Natl Acad Sci USA* 1995, **92**:11264–11268.
6. Nevins J: **Toward an understanding of the functional complexity of the E2F and retinoblastoma families**. *Cell Growth Diff* 1998, **9**:585–593.
7. Kel OV, Kel AE: **Complex gene network in cell cycle regulation: central role of the E2F family of transcription factors**. *Mol Biol* 1997, **31**:656–670.
8. Shan B, Chang CY, Jones D, Lee WH: **The transcription factor E2F-1 mediates the autoregulation of RB gene expression**. *Mol Cell Biol 1994*, **14**:299–309.
9. Pierce AM, Schneider-Broussard, R, Philhower JL, Johnson DG: **Differential activities of E2F family members: unique functions in regulating transcription**. *Mol Carcinogen* 1998, **22**:190–198.
10. Hurford RK Jr, Cobrinik D, Lee M-H, Dyson N: **pRB and p107/p130 are required for the regulated expression of different sets of E2F responsive genes**. *Genes Dev* 1997, **11**: 1447–1463.
11. Brehm A, Miska EA, McCance DJ, Reid JL, Bannister AJ, Kouzarides T: **Retinoblastoma protein recruits histone deacetylase to repress transcription**. *Nature* 1998, **391**:597–601.
12. Magnaghi-Jaulin L, Groisman R, Naguibneva I, Robin P, Lorain S, Le Villain JP, Troalen F, Trouche D, Harel-Bellan A: **Retinoblastoma protein represses transcription by recruiting a histone deacetylase**. *Nature* 1998, **391**:601–604.
13. Ferreira R, Magnaghi-Jaulin L, Robin P, Harel-Bellan A, Trouche D: **The three members of the pocket protein family share the ability to repress E2F activity through recruitment of a histone deacetylase**. *Proc Natl Acad Sci USA* 1998, **95**:10493–10498.
14. Luo RX, Postigo AA, Dean DC: **Rb interacts with histone deacetylase to repress transcription**. *Cell* 1998, **92**:463–473.
15. Lea MA, Randolph VM: **Induction of reporter gene expression by inhibitors of histone deacetylase.** *Anticancer Res* 1998, **18**: 2717–2722.
16. Archer SY, Meng S, Shei A, Hodin RA: **p21^{WAF1} is required for butyrate-mediated growth inhibition of human colon cancer cells**. *Proc Natl Acad Sci USA* 1998, **95**:6791–6796.
17. Richon VM, Emiliani S, Verdin E, Webb Y, Breslow R, Rifkind RA, Marks PA: **A class of hybrid polar inducers of transformed cell differentiation inhibits histone deacetylases**. *Proc Natl Acad Sci USA* 1998, **95**:3003–3007.
18. Richon VM, Webb Y, Merger R, Sheppard T, Jursic B, Ngo L, Civoli F, Breslow R, Rifkind RA, Marks PA: **Second generation hybrid polar compounds are potent inducers of transformed cell differentiation**. *Proc Natl Acad Sci USA* 1996, **93**:5705–5708.
19. Siegel DS, Zhang X, Feinman R, Teitz T, Zelenetz A, Richon VM, Rifkind RA, Marks PA, Michaeli J: **Hexamethylene bisacetamide induces programmed cell death (apoptosis) and down-regulates BCL-2 expression in human myeloma cells**. *Proc Natl Acad Sci USA* 1998, **95**:162–166.
20. Richon VM, Russo P, Venta-Perez G, Cordon-Cardo C, Rifkind RA, Marks PA: **Two cytodifferentiation agent-induced pathways, differentiation and apoptosis, are distinguished by the expression of human papillomavirus 16 E7 in human bladder carcinoma cells**. *Cancer Res* 1997, **57**:2789–2798.
21. Andreeff M, Stone R, Michaeli J, Young CW, Tong WP, Sogoloff H, Ervin T, Kufe D, Rifkind RA, Marks PA: **Hexamethylene bisacetamide in myelodysplastic syndrome and acute myelogenous leukemia: a phase II clinical trial with a differentiation inducing agent**. *Blood* 1992, **80**:2604–2609.
22. Cohen LA, Amin S, Marks PA, Rifkind RA, Desai D, Richon VM: **Chemoprevention of carcinogen-induced mammary tumorigenesis by the hybrid polar cytodifferentiation agent, suberaniohydroxamic acid (SAHA)**. *Anticancer Res* 1999, **19**:4999–5005.
23. Medina D, Kittrell FS, Oborn CJ, Schwartz M: **Growth factor dependency and gene expression in preneoplastic mouse mammary epithelial cells.** *Cancer Res* 1993, **53**:668–674.
24. Jerry DJ, Ozbun MA, Kittrell FS, Lane DP, Medina D, Butel JS: **Mutations in p53 are frequent in the preneoplastic stage of mouse mammary tumor development**. *Cancer Res* 1993, **53**: 3374–3381.
25. Said TK, Medina D: **Interaction of retinoblastoma protein and D cyclins during cell-growth inhibition by hexamethylenebisamide in TM2H mouse epithelial cells**. *Mol Carcinogen* 1998, **22**:128–143.
26. Edmondson DG, Roth SY: **Interactions of transcriptional regulators with histones**. *Methods* 1998, **15**:355–364.
27. Roth SY, Allis CD: **Histone acetylation and chromatin assembly – a single escort, multiple dances**. *Cell* 1996, **87**:5–8.
28. Said TK, Medina D: **Cell cyclins and cyclin-dependent kinase activities in mouse mammary tumor development**. *Carcinogenesis* 1995, **16**:823–830.
29. Liu X, Kim CN, Yang J, Jemmerson R, Wang X: **Induction of apoptotic program in cell-free extracts: requirement for dATP and cytochrome C**. *Cell* 1996, **86**: 147–157.
30. Medina D: **Preneoplasia in mammary tumorigenesis**. In *Mammary Tumor Cell Cycle, Differentiation and Metastases, Advances in Cellular and Molecular Biology of Breast Cancer*. Edited by Dickson RB, Lippman ME. Norwell, MA: Kluwer Academic Publishers, 1996:37–69.
31. O'Keefe RT, Henderson SC, Spector DL: **Dynamic organization of DNA replication in mammalian cell nuclei: spatially and temporally defined replication of chromosome-specific alpha-satellite DNA sequences**. *J Cell Biol* 1992, **116**:1095–1110.
32. Harbour WJ, Luo RX, Dei Santi A, Postigo AA, Dean DC: **Cdk phosphorylation triggers sequential intramolecular interactions that progressively block Rb functions as cells move through G1**. *Cell* 1999, **98**:859–869.
33. Zarkowska T, Mittnacht S: **Differential phosphorylation of the retinoblastaoma protein by G1/S cyclin-dependent kinases**. *J Biol Chem* 1997, **272**:12738–12746.
34. Lundberg AS, Weinberg RA: **Functional interaction of retinoblastoma protein requires sequential modification by at least two distinct cyclin–cdk complexes**. *Mol Cell Biol* 1998, **18**:753–761.
35. Weinberg RA: **The retinoblastoma protein and cell cycle control**. *Cell* 1995, **81**:323–330.
36. Sherr CJ: **G1 phase progression: cycling on cue**. *Cell* 1994, **79**: 551–555.
37. Jonsson ZO, Hubscher U: **Proliferating cell nuclear antigen: more than a clamp for DNA polymerases**. *BioEssays* 1997, **19**:967–975.
38. Jonsson ZJ, Hindges R, Hubscher U: **Regulation of DNA replication and repair proteins through interaction with the front side of proliferating cell nuclear antigen**. *EMBO J* 1998, **17**: 2412–2425.
39. Moberg K, Starz MA, Lees JA: **E2F-4 switches from p130 to p107 and pRb in response to cell cycle reentry**. *Mol Cell Biol* 1996, **16**:1436–1449.
40. Puri PL, Cimino L, Fulco M, Zimmerman C, La Thangue NB, Giordano A, Graessmann A, Levrero M: **Regulation of E2F4 mitogenic activity during terminal differentiation by its heterodimerization partners for nuclear translocation**. *Cancer Res* 1998, **58**:1325–1331.
41. Smith EJ, Leone G, DeGregori J, Jakoi L, Nevins J: **The accumulation of an E2F-p130 transcriptional repressor distinguishes a G0 cell state from a G1 cell state**. *Mol Cell Biol* 1996, **16**:6965–6976.
42. O'Connor PM, Lam EW-F, Griffin S, Zhong S, Leighton LC, Burbidge SA, Lu X: **Physical and functional interactions between p53 and cell cycle co-operating transcription factors, E2F1 and DP1**. *EMBO J* 1995, **14**:6184–6192.
43. Melichar H, Bosch I, Molnar GM, Huang L, Pardee AB: **Detection of eukaryotic cDNA in differential display is enhanced by the addition of *E. coli* RNA**. *Biotechniques* 2000, **28**:76–82.
44. Struhl K: **Histone acetylation and transcriptional regulatory mechanisms**. *Gene Dev* 1998, **12**:599–606.
45. Lint CV, Emiliani S, Verdin E: **The expression of a small fraction of cellular genes is changed in response to histone hyperacetylation**. *Gene Expression* 1996, **5**:245–253.

46. Johnson DG, Ohtani K, Nevins JR: **Autoregulatory control of E2F1 expression in response to positive and negative regulators of cell cycle progression**. *Gene Dev* 1994, **8**:1514–1525.
47. Zhu L, Xie E, Chang LS: **Differential roles of two tandem E2F sites in repression of the human p107 promoter by retinoblastoma and p107 proteins**. *Mol Cell Biol* 1995, **15**:3552–3562.
48. Richon VM, Sandhoff, TW, Rifkind RA, Marks PA: **Histone deacetylase inhibitor selectively induces p21^{WAF1} expression and gene-associated histone acetylation**. *Progr Natl Assoc Sci* 2000, **97**:10014–10019.
49. De la Luna S, Burden MJ, Lee C-W, La Thangue NB: **Nuclear accumulation of the E2F heterodimer regulated by subunit composition and alternative splicing of a nuclear localization signal**. *J Cell Sci* 1996, **109**:2443–2452.
50. Magae J, Wu C-L, Illenye S, Harlow E, Heintz NH: **Nuclear localization of DP and E2F transcription factors by heterodimeric partners and retinoblastoma protein family members**. *J Cell Sci* 1996, **109**:1717–1726.
51. Ikeda M-A, Jakoi L, Nevins JR: **A unique role for the Rb protein in controlling E2F accumulation during cell growth and differentiation**. *Proc Natl Acad Sci USA* 1996, **93**:3215–3220.
52. Cobrinik D, Whyte P, Peeper DS, Jacks T, Weinberg RA: **Cell cycle-specific association of E2F with the p130 E1A-binding protein**. *Gene Dev* 1993, **7**:2392–2404.
53. Gu W, Roeder RG: **Activation of p53 sequence-specific DNA binding by acetylation of the p53 C-terminal domain**. *Cell* 1997, **90**:595–606.
54. Sakaguchi K, Herrera JE, Saito S, Miki T, Bustin M, Vassilev A, Anderson CW, Appella E: **DNA damage activates p53 through a phosphorylation-acetylation cascade**. *Gene Dev* 1998, **12**:2831–2841.
55. Chiarugi V, Cinelli M, Magnelli L: **Acetylation and phosphorylation of the carboxy-terminal domain of p53: regulative significance**. *Oncol Res* 1998, **10**:55–57.
56. Weiss RH Randour CJ: **The permissive effect of p21(Waf1/Cip1) on DNA synthesis is dependent on cell type. Effect is absent in p53-inactive cells**. *Cell Signal* 2000, **12**:413–418.
57. Shi YZ, Hui AM, Takayama T, Li X, Cui X, Makuuchi M: **Reduced p21(WAF1/Cip1) protein expression is predominantly related to altered p53 in hepatocellular carcinomas**. *Br J Cancer* 2000, **83**:50–55.